**Supplementary Information**

This document contains the synthetic schemes of TESP-BT, TESP-BT-SG and APTES-SG, as well as the procedure outlining the batch adsorption method. Characterization techniques including 1-D and 2-D NMR, FTIR, mass spectra together with the TGA-DTA and pK_a/pK_b graphs are also presented. Tables reporting the BET, XRF, loading capacities results and stacked adsorption efficiency graphs of the adsorbents are also included.
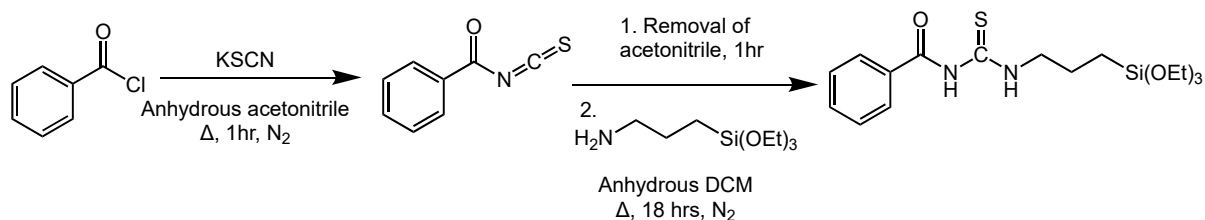
Scheme S1. *Synthesis of N,N-di(trimethoxysilylpropyl)-N'-benzoylthiourea.*
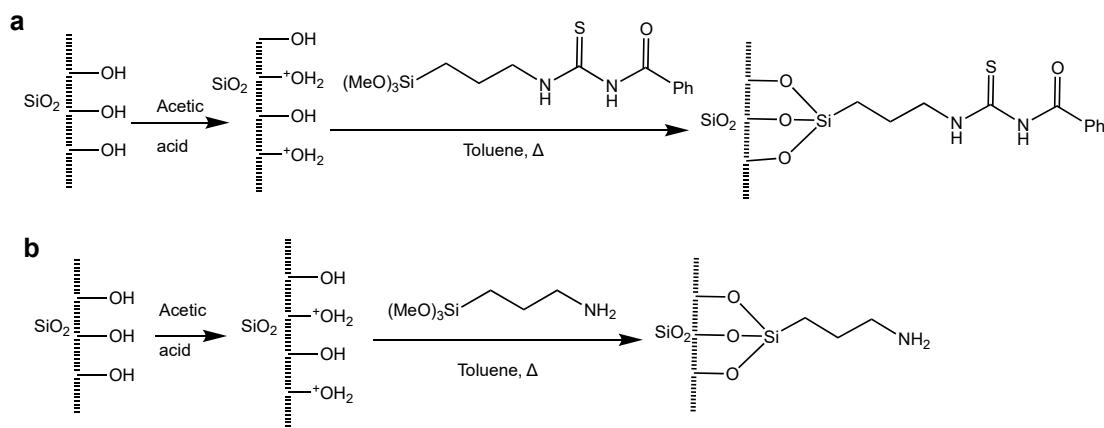
Scheme S2. *Reaction schemes for the functionalization of silica gel with a) TESP-BT and b) APTES.*
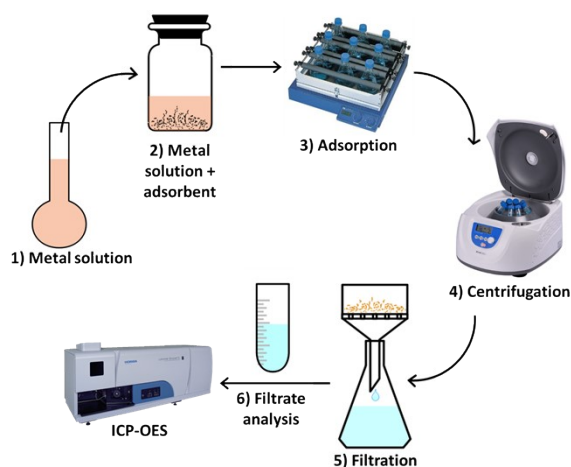

Figure S1. *Batch adsorption procedure for recovery of Pt and Pd from aqueous solutions.*
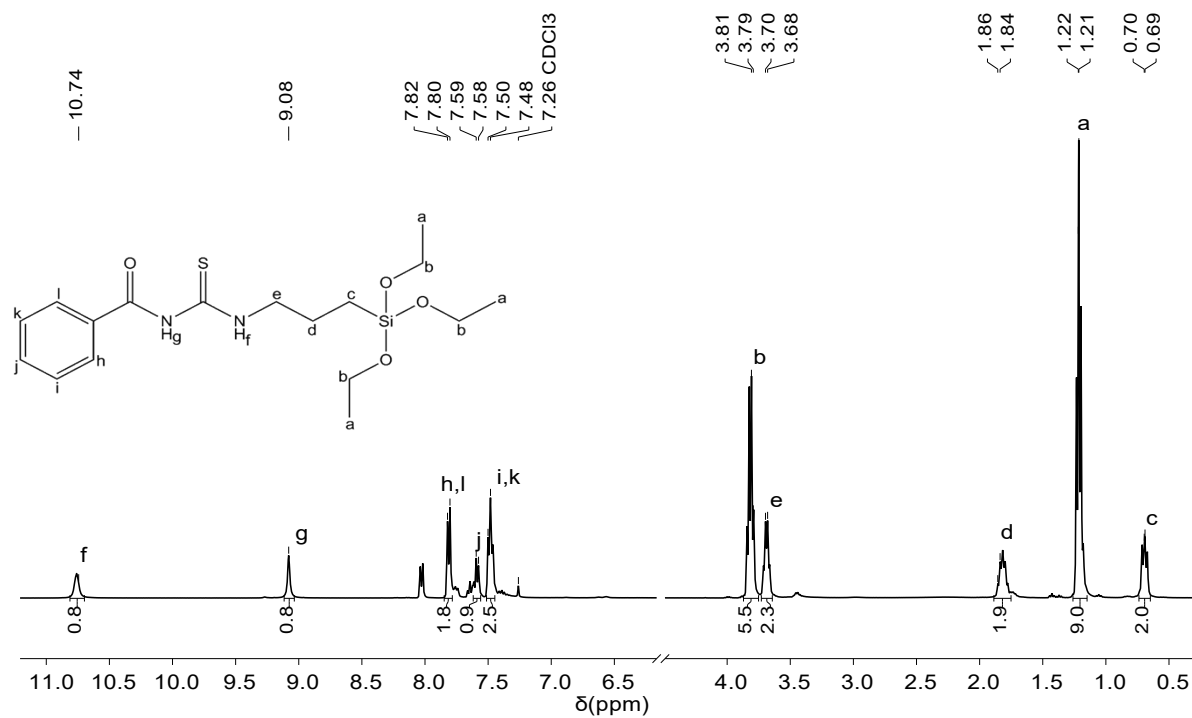
Figure S2. ^1H NMR spectrum of TESP-BT in CDCl$_3$ at 25°C. (Note the break in scale between
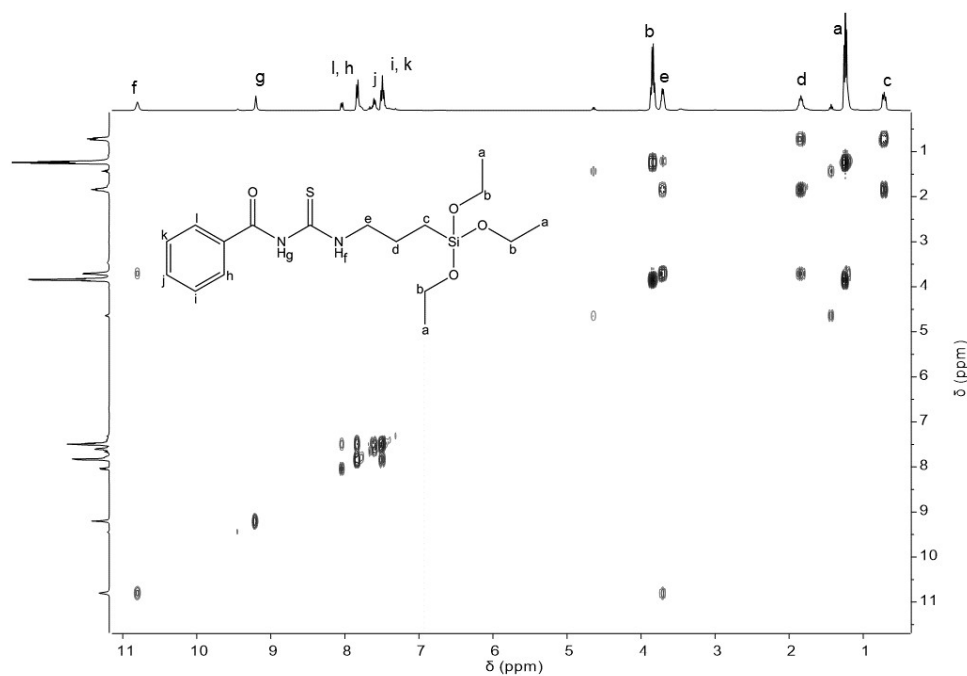
4.0–6.5 ppm.
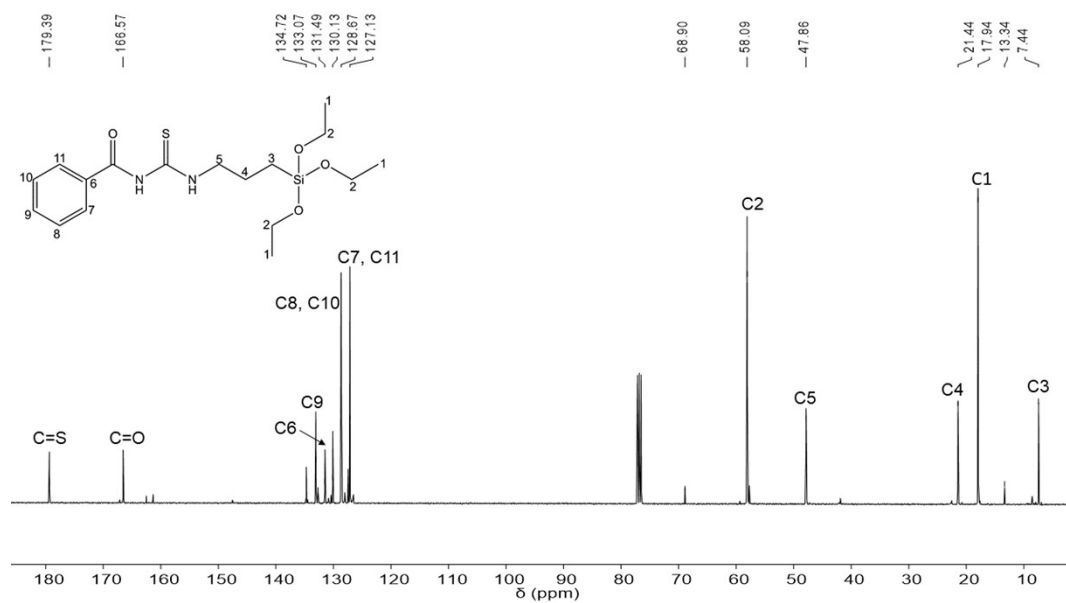

Figure S3. The 2D COSY spectrum of TESP-BT in CDCl$_3$ at 25°C.

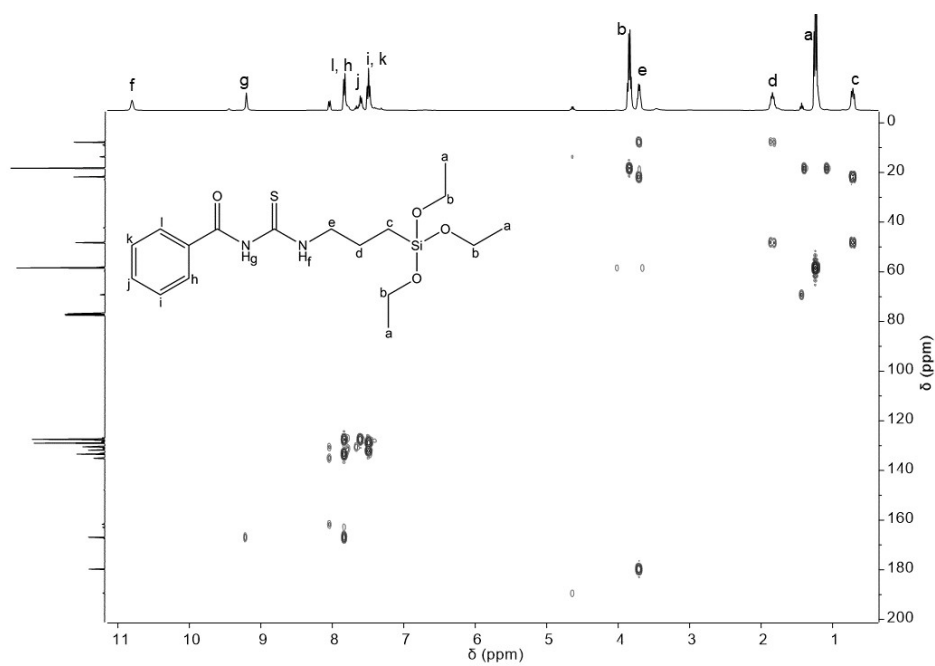**Figure S4**. ^{13}C spectrum of TESP-BT in CDCl$_3$ at 25°C with impurities marked.

Fig

ure S5. The 2D HMBC spectrum of TESP-BT in CDCl$_3$ at 25°C.
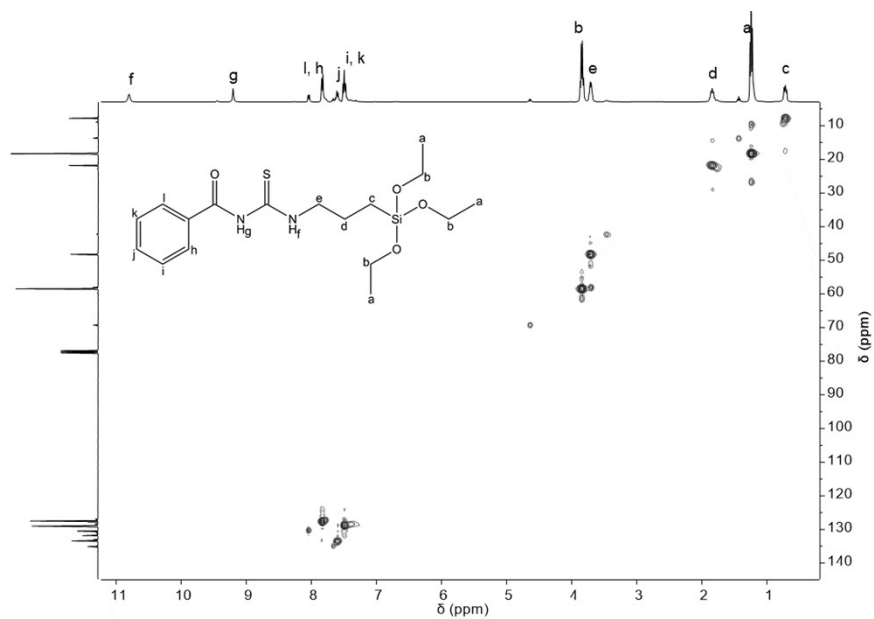
Figure S6. *The 2D HSQC spectrum of TESP-BT in CDCl₃ at 25°C.*
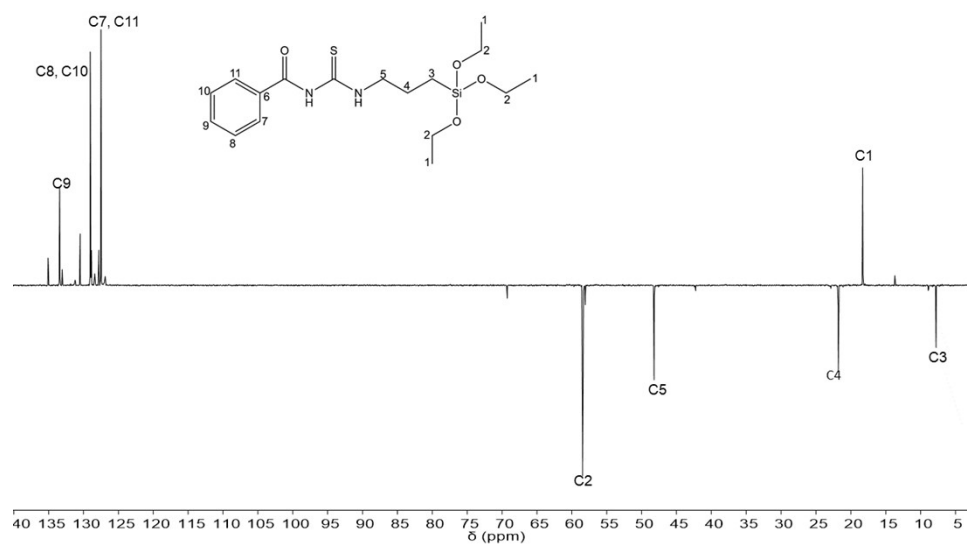
Figure S7. *¹³C DEPT Spectrum of TESP-BT in CDCl₃ at 25°C.*
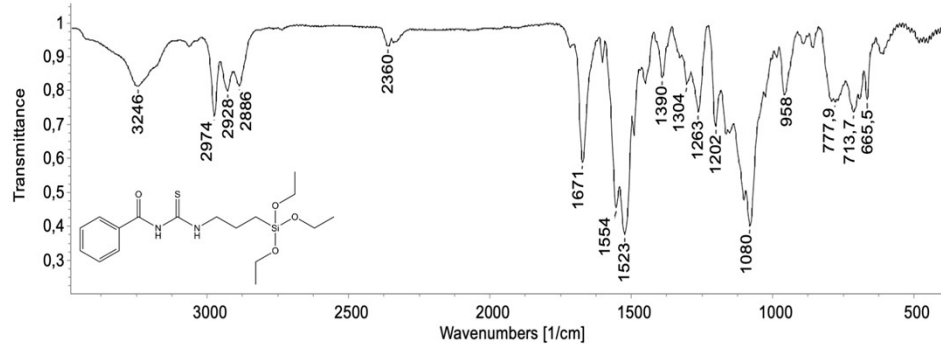
Figure S8. *FT-IR Spectroscopy spectrum TESP-BT.*

Figure S9. *Mass Spectrometry spectrum of TESP-BT.*

Figure S10. *FT-IR Spectroscopy spectrum ATPES-SG.*

Table S1. *Textural properties of the adsorbents.*

	Pore size (nm)	Pore volume (cm^3 g^{-1})	Surface area (m^2 g^{-1})
Silica gel	6.47	0.94	451.25
TESP-BT-SG	5.93	0.62	322.18
APTES-SG	7.42	0.45	180.19

Table S2. *XRF Chemical compositions of the adsorbents.*
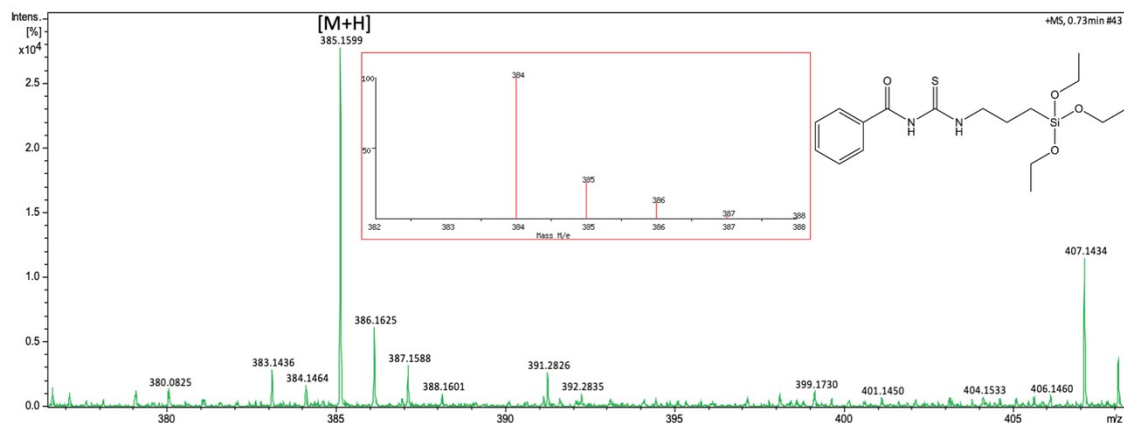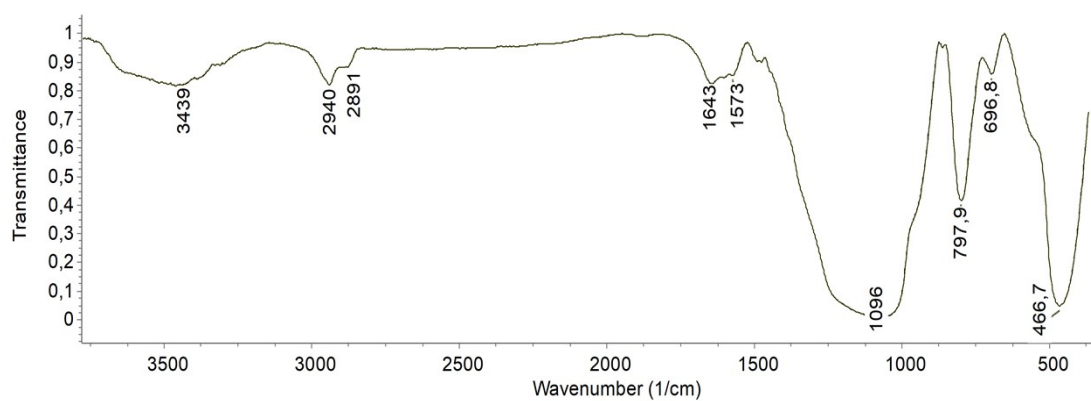
	Silica gel	TESP-BT-SG	APTES-SG
Compounds	Percentage composition (wt.%)		
SiO_2	89.20	78.81	79.41
Al_2O_3	0.09	0.08	0.07
Fe_2O_3	-0.03	-0.03	-0.02
MnO	0	0	0
MgO	0.02	0.02	0.02
CaO	0.07	0.07	0.1
Na_2O	0.07	0.02	0.03
K_2O	-0.03	-0.02	0
TiO_2	0.03	0.02	0.02
P_2O_5	0.04	0.01	0.01
Cr_2O_3	-0.01	0	0
NiO	0	0	0
Loss on Ignition (LOI)	9.67	19.45	20.31
TOTAL	99.12	98.41	99.93
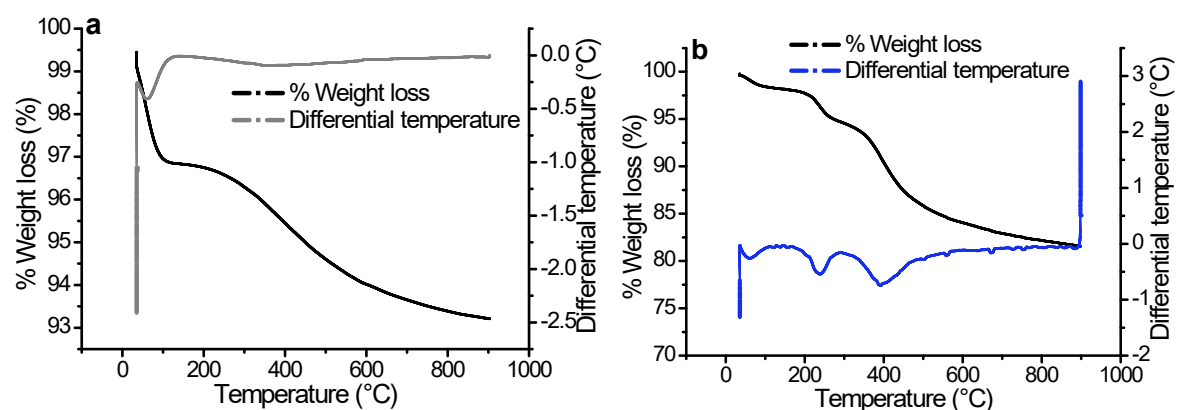
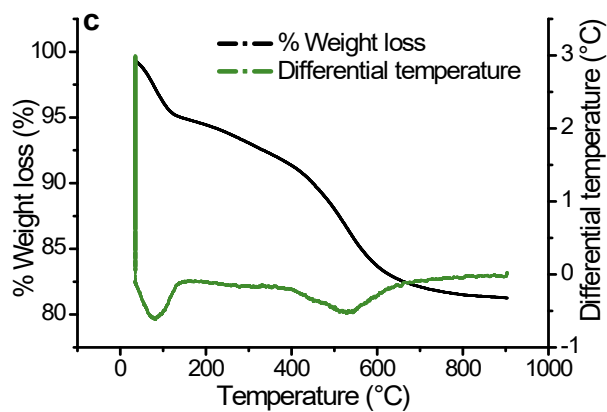**Figure S11.** *TGA and DTA graphs of a) Silica gel, b) TESP-BT-SG and c) APTES-SG.*
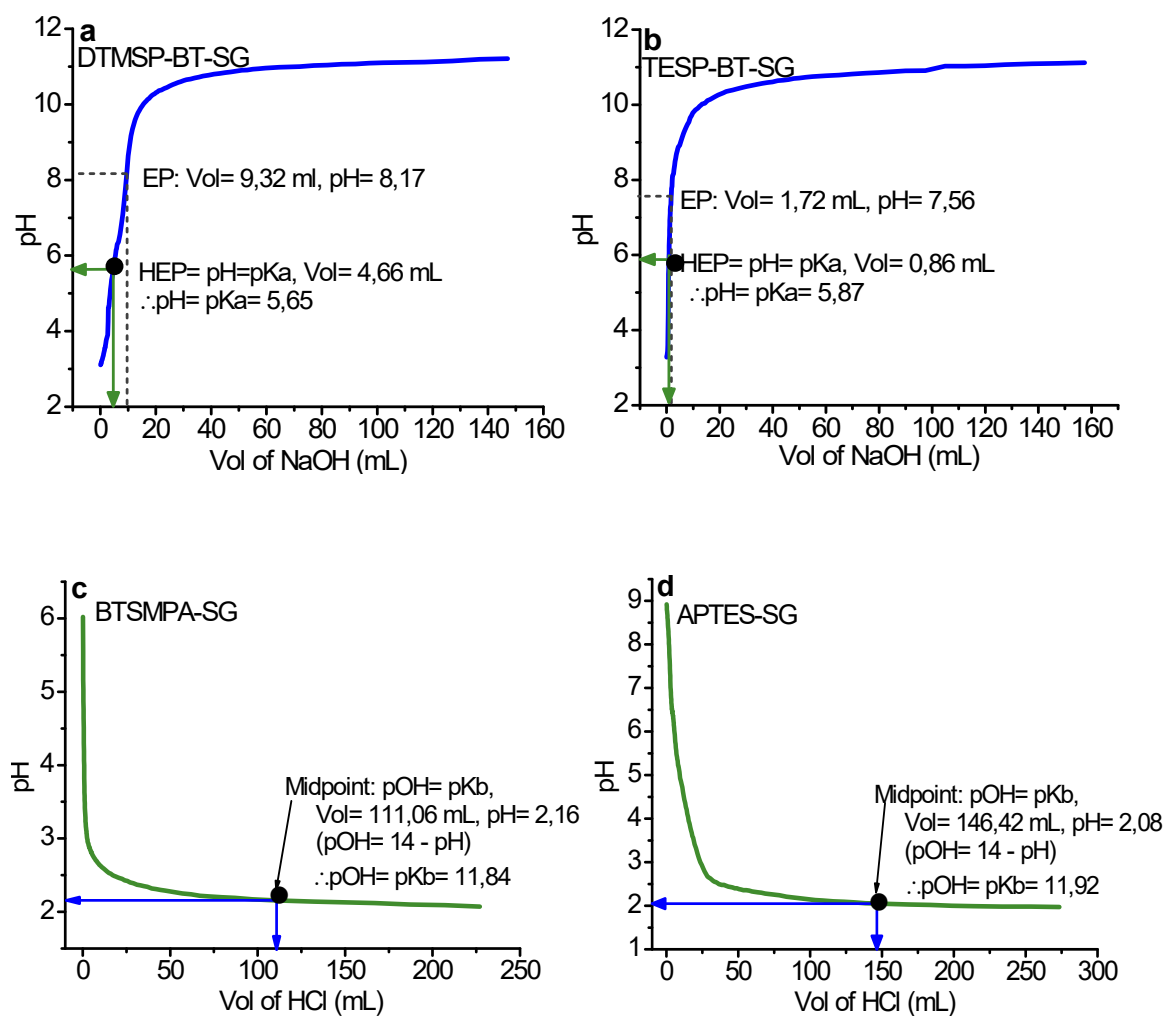

Figure S12. pK_a and pK_b plots of the adsorbents.

Table S3. *The Pt and Pd theoretical and experimental loading capacities obtained from CHNS data (based on N content) and from the Langmuir isotherm model.*

	Metal	Theoretical q_{max}	Experimental q_{max}		Ligand conc. (N)	Ligand: metal ratio	Volume of max adsorption
		mg g^{-1}	mg g^{-1}	mmol g^{-1}			mL
TESP-	Pt	107.88	29.01	0.149	0.553	3.72	58.02
BT-SG	Pd	58.85	28.66	0.269	0.553	2.05	57.32
APTES-	Pt	477.56	25.06	0.128	2.448	19.06	50.12
SG	Pd	260.52	32.73	0.308	2.448	7.96	65.46
Previous work[17]							
DTMSP-	Pt	201.13	48.52	0.249	1.03	4.15	97.04
BT-SG	Pd	109.72	29.68	0.279	1.03	3.69	59.36
BTMSPA	Pt	329.55	6.63	0.034	1.68	49.36	13.26
-SG	Pd	179.77	12.53	0.118	1.68	14.24	25.06

Table S4. *The loading capacities of commonly known adsorbents.*[38,39]

| Adsorbents	$q_{max)}$ (mg/g)		Ref.
	Pt	Pd	
TESP-BT-SG	29.01	28.66	This
APTES-SG	52.77	32.73	work
DTMSP-BT-SG	48.52	29.68	Prev.
BTMSPA-SG	6.63	12.53	work[17]
Amberlite IRC 718	66.33	58.52	39
2-Mercaptobenzothiazole-bonded silica gel	6.50	18.00	40
Ethyl-3-(2-aminoethylamino)-2-chlorobut-2-enoate modified activated carbon	126.0	92.0	38
Fe_3O_4 nanoparticles	13.27	10.96	41
Bayberry tannin immobilized collagen fibre membrane	45.80	33.40	38
(E,E,E)-1-[(4-methylphenyl)sulfonyl]-6-[(2-trimethylsilylethyl)sulfonyl]-11-[(4-vinylphenyl)sulfonyl)]-1,6,11-triazacyclopentadeca-3,8,13-triene functionalized polystyrene	54.62	38.31	42
Glycine-modified chitosan	122.47	120.39	43
Thiourea-modified chitosan	129.87	112.36	39
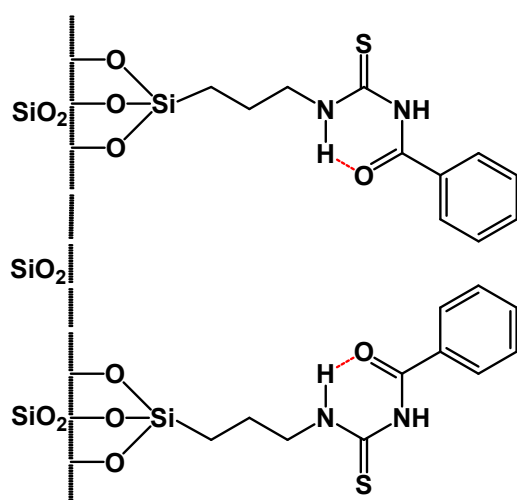
Figure S13. *TESP-BT-SG adsorbent structure with intramolecular hydrogen bonding highlighted in red.*